Clinics in Oncology

Research Article
Published: 16 Oct, 2018

Guar Gum Stabilized Gold Nanoparticles for Colon Cancer Treatment

*Moorthy Ganeshkumar[1], Murthi Janani[2], Thangavel Ponrasu[1] and Lonchin Suguna[1]**

[1]Department of Biochemistry and Biotechnology, CSIR-Central Leather Research Institute, India

[2]Department of Biopharmaceutics, Anna University, India

Abstract

In this study, microwave irradiated gold Nanoparticles were prepared using guar gum, a biopolymer, and utilized for targeted drug delivery for colon cancer for the first time. Guar gum stabilized gold Nanoparticles (GG-AuNPs) thus prepared, observed to possess hemocompatibility. 5-Fluorouracil (5-Fu), an anti-cancer drug, was adsorbed on GG-AuNPs (5-Fu@GG-AuNPs) and used for targeted drug delivery for colon cancer. The toxicity and angiogenesis of 5-Fu, 5-Fu@GG-AuNPs was studied using zebrafish embryos. The cytotoxicity of free 5-Fu, 5-Fu@GG-AuNPs was carried out on HT-29 cells and found that the amount of 5-Fu required to achieve 50% of growth of inhibition (Ic_{50}) was higher in 5-Fu@GG-AuNPs than in 5-Fu, due to a slow release of drug from Nanoparticles.

Keywords: Gaur gum; Gold nanoparticles; Zebra fish; Colon cancer; Drug delivery

Introduction

Nanoparticles have become an important area of research in the field of targeted drug delivery as they have the ability to deliver the drug to targeted area with sustained period of time with limited side effects in the non targeted areas [1]. Gold Nanoparticles (AuNPs) are drawing lot of interest and attention as a new platform for biomedical applications, than any other metallic Nanoparticles due to their biocompatibility and non-cytotoxicity [2-3]. In clinical applications, the advantage of AuNPs is that they can be readily conjugated to many bio molecules like amino acids, proteins/enzymes, DNA [4-6] and other molecular species without altering the biological activity of the conjugated species. Functionalized AuNPs has opened the door wide to biomedical applications such as colorimetric assays of amoxicillin [7], creatinin [8], melanin [9], bio-sensing [10] and drug delivery [11]. Recently, we have reported a method for spontaneous ultra fast synthesis of gold nanoparticles using *Punica granatum* for cancer targeted drug delivery [12]. Green synthesis of pullulan stabilized gold nanoparticles for cancer targeted drug delivery for the treatment of liver cancer has also been reported by us [13]. Until now, varieties of methods or techniques have been reported for the preparation of AuNPs [14-16]. One of the most commonly used methods is the chemical reduction of gold salts by various reducing agents, such as sodium borohydride, sodium citrate, form amide [17-18]. Sodium borohydride is toxic to human. As citric acid reduced AuNPs are not stable in physiological conditions, synthesis of AuNPs needs protective or stabilizing agents such as thiols, surfactants and polymers, which can attach to the surface of AuNPs, and thus preventing the agglomeration [19-22]. Green chemistry based synthesis of gold Nanoparticles could tackle the above problem and could be used for targeted drug delivery due to their biocompatibility and stability in physiological conditions.

Oral controlled drug delivery systems based on natural hydrophilic polysaccharides are highly appreciable due to their economic feasibility, controlled drug release and regulatory acceptance. Guar Gum (GG) is a high molecular weight (2, 20000 Daltons) hydro-colloidal polysaccharide derived from the seeds of *Cyamopsis tetragonolobus*. The gum consists of linear chains of (1→4)-β-D-mannopyranosyl units with α-D-galactopyranosyl units attached by (1→6) linkages [23]. The pH of 1% (w/v) aqueous dispersion varies from 5 to 7 and is stable over a wide pH range. The viscosity of GG dispersion is same in both acidic and alkaline media. In pharmaceuticals, guar gum is used as a binder and disintegrant in solid dosage forms [24].

GG is generally considered as a potential candidate for colon-specific drug delivery application due to its drug release retarding property and susceptibility to microbial degradation in the large intestine [25-26]. Gamma scintiographic studies on GG matrix tablets in human models showed that they are appropriate carriers for colon region [27]. Carboxymethyl gaur gum stabilized

OPEN ACCESS

Correspondence:
Lonchin Suguna, Department of Biochemistry and Biotechnology, CSIR-Central Leather Research Institute, India, Tel: (+) 91-44-24437149; Fax: (+) 91-44-24911589; E-mail: slonchin@yahoo.co.uk

Received Date: *18 Sep 2018*
Accepted Date: *05 Oct 2018*
Published Date: *16 Oct 2018*

Citation:
Ganeshkumar M, Janani M, Ponrasu T, Suguna L. Guar Gum Stabilized Gold Nanoparticles for Colon Cancer Treatment. Clin Oncol. 2018; 3: 1539.

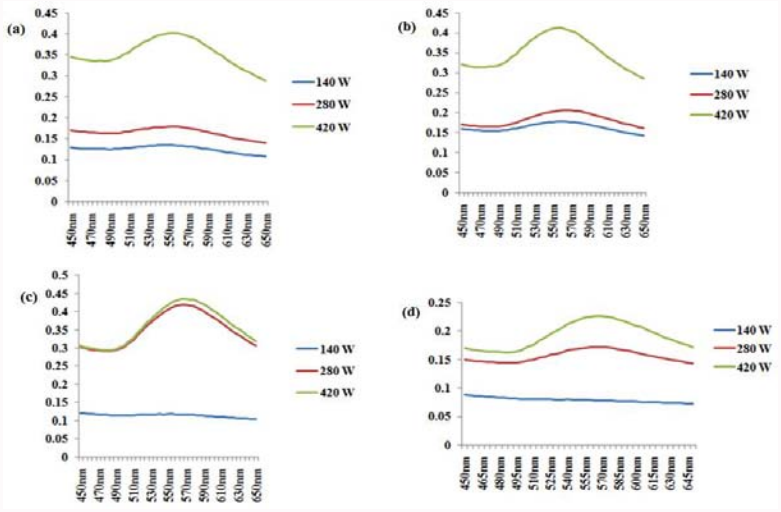

Figure 1: UV–Vis spectra of GG-AuNPs synthesized with different microwave powers and concentration of guar gum. (a) 1% guar gum, (b) 0.5% guar gum, (c) 0.25% guar gum and (d) 0.0625% guar gum.

Nanoparticles were prepared and studied for their cytotoxicity [28].

5-Fu has a long history of usage as a chemotherapeutic agent. This pyramidine analogue interferes with thymidylate synthesis and acts against solid tumors [29-31]. Presently, only intravenous preparations of 5-Fu are available in market for clinical use which has been reported to cause severe gastrointestinal, dermatological, hematological, cardiac and neurological side effects due to the distribution in non-targeted area [32].

Longer exposure to lower concentration of 5-Fu has been reported to favor DNA-directed effects which is thought to contribute to its anti tumor activity [33]. Colon-specific delivery systems would allow the local delivery of a high concentration of 5-Fu in the colon to improve pharmacotherapy and reduce its potential systemic toxicity and side effects [34-35]. Gajalakshmi et al. have reported the synthesis and characterization of copper oxide nanofluids by one step chemical method using guar gum as stabilizer [36]. The copper oxide nanofluid thus prepared showed high antibacterial activity equivalent to that of streptomycin. Balachandramohan et al. have reported a simple method for the synthesis of Fe_3O_4-guargum nanocomposites for treating environmental pollutants [37].

Even though, there are several papers available on gaur gum stabilized metal Nanoparticles, the role of gaur gum stabilized gold Nanoparticles on colon cancer is not yet studied. Hence in this paper, we have reported a new one step rapid synthesis of AuNPs by microwave irradiation using GG for the first time. GG contains galactomannan backbone that has high specificity to galectine 1-s lectine receptor which is over expressed in colon cancer cell [1]. Galactomannon functionalized nanoparticle adsorbed 5-Fu can easily penetrate the cancer cells due to receptor specific binding. It is thus hypothesized that targeted delivery of 5-Fu by GG stabilized gold Nanoparticles through oral route may tackle the problems of the usual conventional delivery system and improve the patient compliance.

Materials and Methods

Materials

Hydrogen tetra chloroaurate (III) ($HAuCl_4$) was purchased from Sigma Aldrich. GG was obtained from Hi-Media. All other chemicals were of analytical grade and used without further purification.

Synthesis of GG-stabilized AuNPs (GG-AuNPs)

For optimizing the AuNPs formation, 300µl of $HAuCl_4$ solution (1×10^{-4} M) was added to various concentration of GG (1%, 0.5%, 0.25%, 0.125%, and 0.0625%) and placed in a microwave oven. Then the reaction mixture was irradiated by microwave in a predesigned mode. In the reduction process, some experimental parameters such as microwave power (140, 280, 420 watts) and irradiation time (30, 60, 90, 120, 150, 180 sec) were adjusted to investigate their effect on the formation of AuNPs. The formation of AuNPs was confirmed by UV–Vis spectra.

The optimized nanoparticle solution was centrifuged at 12,000 rpm for 20 min. Then the pellets were re dispersed in distilled water for further characterization.

Characterization of AuNPs and 5-Fu loaded AuNPs

The change in surface plasmon resonance of AuNPs, before and after microwave irradiation, was monitored by UV/Vis/NIR spectroscopy measurements, carried out on a Infinite M200, TECAN. Fourier Transform Infrared (FTIR) spectra of GG, GG reduced AuNPs, 5-Fu and 5-Fu loaded AuNPs were recorded using Perkin Elmer Fourier Transformation Infrared Spectroscopy. The scan was performed in the range 4000-400 cm^{-1}. Surface morphology of GG-AuNPs was carried out on Techni-20 Philips transmission electron microscope operated at 80 kev. TEM samples were prepared by the dispersion of 2–3 drops of GG-AuNPs solution on a copper grid and dried at room temperature after removal of excess solution with filter paper. The particle size and distribution of drug-loaded AuNPs were elucidated by ZETASIZER (Malvern Instruments, Germany).

Preparation and adsorption efficiency of 5-Fu@GG-AuNPs

A calculated amount of 5-Fu (10 mg/ml) was added to GG-AuNPs solution, stirred for 24 hr at room temperature and then centrifuged at 12,000 rpm for 20 min. The drug concentration in supernatant was quantified by measuring at 266 nm in a UV-visible spectrophotometer. The percentage loading of 5-Fu onto GG-AuNPs was calculated using the following formula.

$$\text{Loading efficiency} = \frac{\text{Amount of drug added during preparation} - \text{Amount of drug in the supernatant}}{\text{Amount of drug added during preparation}} \times 100$$

Stability study of AuNPs

The stability of GG-AuNPs was checked at different physiological

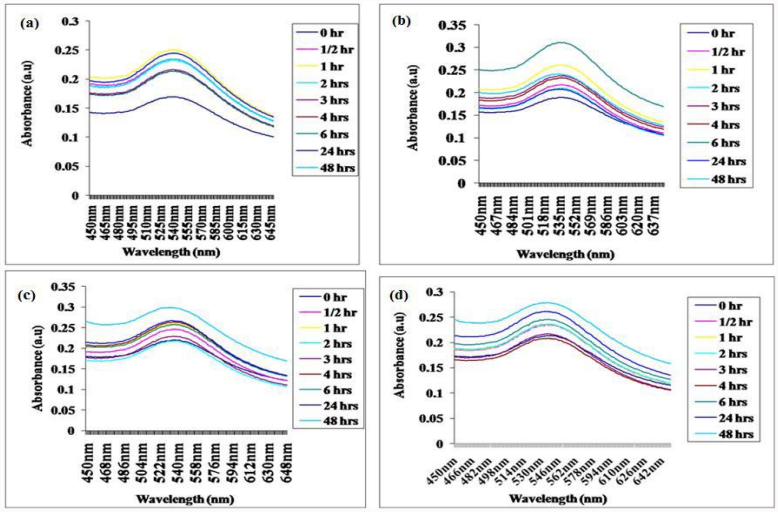

Figure 2: UV-Visible absorption spectrum showing *in vitro* stability of GG-AuNPs at 48 hr in various buffer (a) pH 1.2, (b) pH 4.5, (c) pH 6.8 and (d) pH7.4.

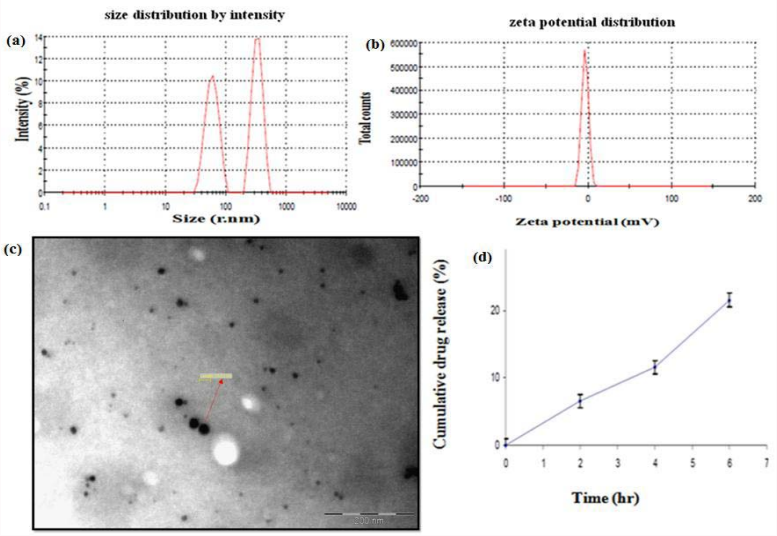

Figure 3: (a) Particle size analysis of 5-Fu@GG-AuNPs, (b) Zetapotential of 5-Fu@GG-AuNPs, (c) TEM image of GG-AuNPs and (d) *In vitro* drug release of 5-Fu@GG-AuNPs. The average particle size of 5-Fu@GG-AuNPs by DLS was found to be 588.1 nm as seen in Figure 3a. The increase in particle size is because of the coating of the particles by the water swellable guar gum. But Uv-visible spectra of GG-AuNPs showed an average particle size of 82 nm due do surface plasmon resonance of gold core nano particles. Figure3b shows the zeta potential value of 5-Fu loaded polymer stabilized a gold nano particle which was found to be -3.18 (mV). TEM images show (Figure 3c) the external morphology of GG-AuNPs. The particles were found to be uniform in size and spherical in shape (black spots). The mean particle size of GG-AuNPs by TEM was found to be 12.78 ± 4.26 nm.

pH like 1.2, 4.5, 6.8 and 7.4. The change in Surface Plasmon Resonance (SPR) was recorded up to 48 hr.

In-vitro drug release characteristics

A polymer complex was prepared using alginate and chitosan in the ratio of 7:3. GG-AuNPs loaded with 5-Fu was dispersed in this polymer mixture. 100 µl of 1 M barium chloride (chelating agent) was added to the polymer mixture, in order to obtain hydrogel [38]. *In vitro* release studies of GG-AuNPs loaded with 5-Fu was performed by taking the 5-Fu@GG-AuNPs in 50 ml of pH 7.4 buffer solutions. Aliquots was withdrawn periodically and replaced with fresh buffer. 5-Fu content in the aliquots was assayed in UV/Visible spectrophotometer at 266 nm.

Hemocompatibility of human blood for the GG-AuNPs [39]

To measure the hemocompatibility of GG-AUNPs blood was collected from a healthy donor with permission. Blood collected in heparinized tubes was centrifuged at 1600 rpm for 10 min at 37°C. The pellet with Red Blood Cells (RBC) was washed twice with PBS. Different concentrations of the GG-AuNPs were added to 500 µl of erythrocyte suspension and made up to 1ml with PBS. The tubes were gently mixed in a rotary shaker and then incubated for 4 hr at 37°C. The serum was collected after centrifugation at 12000 rpm for 20 min. The release of hemoglobin into the supernatant was estimated using Spectrophotometer at 575 nm. Distilled water was used as the positive control and PBS was used as the negative control. Each experiment was performed in duplicates. The percentage of hemolysis was calculated according to the formula given below.

$$\%\ \text{hemolysis} = \frac{\text{OD of test} - \text{OD of negative control}}{\text{OD of positive control} - \text{OD of negative control}} \times 100$$

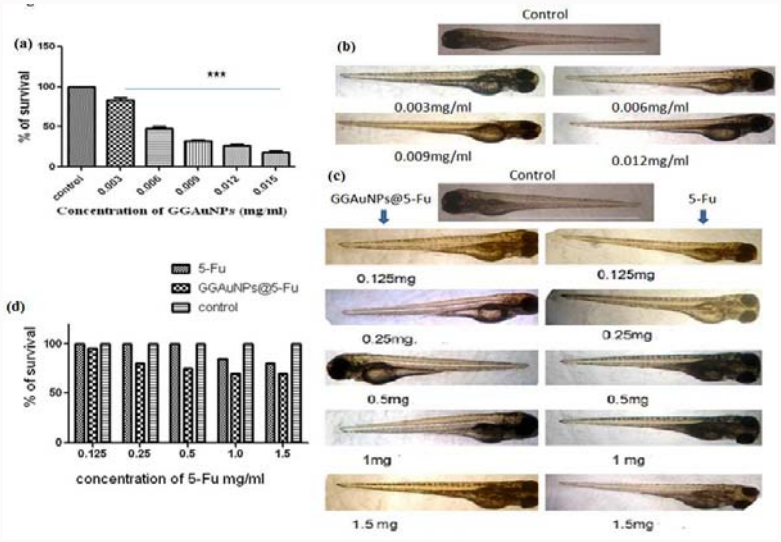

Figure 4: (a) Graph representing the toxicity of GG-AuNPs in terms of survival rate of larvae. Each bar represents the mean ± SD of triplicate experiments. Significant differences compared to controls are indicated by ***p<0.001 and were calculated with one-way ANOVA and Dunnett's post-test. (b) Morphologic analysis of GG-AuNPs toxicity, (c) Graph representing the toxicity of 5-Fu and 5-Fu@GG-AuNPs in terms of survival rate of larvae and (d) Morphological analysis of 5-Fu@GG-AuNPs and 5-Fu toxicity.

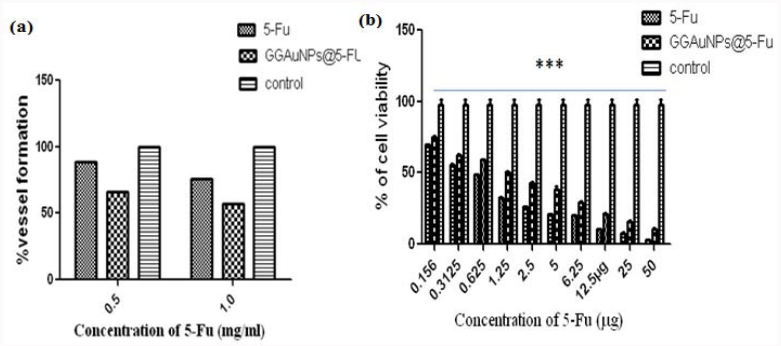

Figure 5: (a) Anti-angiogenic activity of 5-Fu@GG-AuNPs was compared with 5-Fu using zebrafish angiogenic assay and (b) The cytotoxicity of free 5-Fu, 5-Fu@GG-AuNPs, against HT-29 cells. Figure 5 (a) and (b) each bar represent the mean ± SD of triplicate experiments. Significant differences compared to controls are indicated by ***p<0.001 and were calculated with two way ANOVA followed by bonferroni test.

In vivo toxicity study of GG-AuNPs, 5-Fu, 5-Fu@GG-AuNPs in zebrafish embryo model

Fertilized eggs of zebrafish were obtained from natural mating of adult zebrafish and embryos were collected within 2 hr of spawning. From the newly fertilized eggs, approximately 2 hr post fertilization (hpf), 10 healthy embryos were transferred to each wells of a 24 well plate along with 1 ml of E3 medium. The embryos were exposed to different concentration of GG-AuNPs (0.003 mg, 0.006 mg, 0.009 mg, 0.012 mg, and 0.015 mg), 5-Fu (0.125 mg, 0.25 mg, 0.5 mg, 1 mg, 1.5 mg), 5-Fu@GG-AuNPs (0.125 mg, 0.25 mg, 0.5 mg, 1 mg, 1.5 mg) for 4 days, tests were performed in duplicate.

Quantitative endogenous alkaline phosphatase assay on zebrafish embryo

10 healthy embryos were transferred to each wells of a 24 well plate along with 1 ml of E3 medium containing PTU (1-phenyl-2-thiourea) to a final concentration of 0.2 mM before drug administration. At 24 hpf, embryos were treated with two concentrations of drug (0.5 and 1.5 mg). After 72 hr, the drug-treated embryos were dehydrated by increasing concentration of methanol in PBS (25%, 50%, 75% and 100%). Then the embryos were washed twice with PBS. The embryos were stained according to the protocol described in phosphatase substrate kit. After staining, 2M NaOH was added to stop the reaction. The optical density of soluble end product was measured at 405 nm. Vessel growth was calculated as percentage by measuring the changes in optical density compared with control [40].

$$\%\ \text{vessel formation} = \frac{\text{OD treated day 3} - \text{OD control day 1}}{\text{OD control day 3} - \text{OD control day 1}} \times 100$$

Cytotoxicity of 5-Fu, 5-Fu@GG-AuNPs in HT-29 cell Line

HT-29 cells were seeded in 96 well plates with a cell density of 50000 cells/well and incubated at 37°C. After 24 hr, the cells were treated with different concentrations of 5-Fu, 5-Fu@GG-AuNPs. After 48 hr, MTT was added to the cells and incubated for 4 hr at 37°C. The purple color formazan crystals were solubilized and measured at 570 nm.

Results and Discussion

Optimization and synthesis of GG-AuNPs

UV–Vis spectra of GG-AuNPs synthesized with different microwave powers and concentration of GG are shown in Figure 1. UV–Vis spectra confirm the formation of AuNPs, which is clearly evident from the SPR absorption band centering at 555 nm. However, it should be noted that as the change in the microwave powers applied, the intensities of SPR peaks in the UV–Vis spectra also changed

Table S1: Hemocompatibility of GG-AuNps.

Sample	% Hemolysis
Positive control-water	99.8 ± 0.2
Negative control-PBS	0
0.006 mg/ml	0.1928 ± 0.2
0.0012 mg/ml	0.3571 ± 0.1
0.0018 mg/ml	0.8571 ± 0.0

Values are expressed as mean ± SD (n=3).

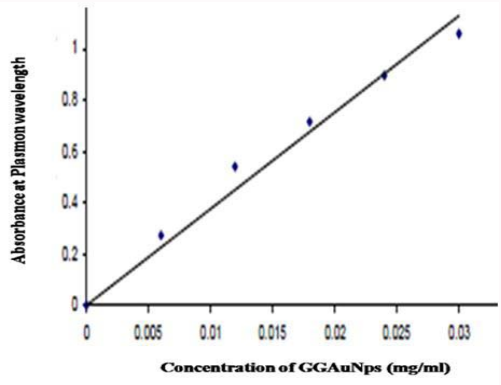

Figure S1: (a) Shows concentration dependent absorbance at Plasmon wave length of GG-AuNPs.

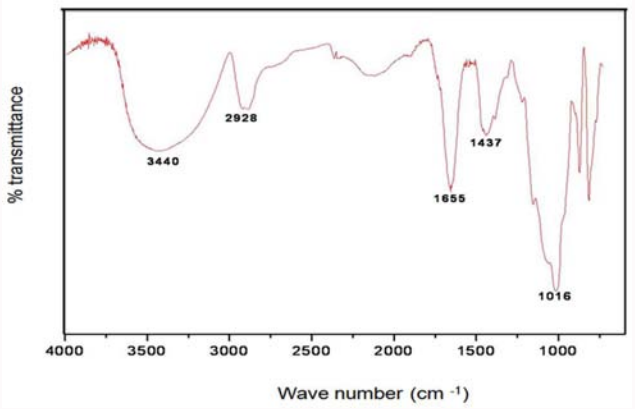

Figure S2: FTIR spectrum of guar gum reduced gold nano particles GG-AuNPs .

suggesting that the formation of AuNPs depends on the power and concentration of GG as observed in Figure 1. Even though, 0.5% and 1% GG showed SPR peaks at 555 nm, the absorption intensities varied from 0.4015 to 0.413 respectively. Further reducing the concentration of GG to 0.25% and 0.0625%, the SPR peaks shifted to 565 nm with an absorption intensity of 0.4351 and 0.2225 respectively. Typically, when microwave power of 420 w was applied to 0.5% GG, the AuNPs could be rapidly synthesized within 3 min, and the resulting solution was deep purple in color. GG acts as a stabilizing agent and microwave irradiation helps in the formation of Nanoparticles with high yield and great reproducibility and increased reaction kinetics.

Stability of GG-AuNPs

The stability of AuNPs in biological fluids over a reasonable period of time is an important issue [41]. The *in vitro* stability of GG-AuNPs was evaluated by monitoring the Plasmon wavelength (λ_{max}) in simulated gastro-intestinal fluids with pH 1.2, 4.5, 6.8 and 7.4 for 48 h which are shown in Figure 2a, 2b, 2c and 2d respectively.

The λ_{max} in all the above fluids showed minimal shift of ~10 nm. This stability study confirmed that the GG-AuNPs were intact and possessed exceptional *in vitro* stability in simulated fluids of different physiological pH. Concentration of gold Nanoparticles is a key factor for biomedical applications. It is important to ensure that λ_{max} of the GG-AuNPs should not change at different dilutions. In order to obtain the stability of GG-AuNPs under various dilutions, the λ_{max} was monitored after the addition of distilled water to various concentrations of GG-AuNPs and made up the volume to 0.5 ml. The absorbance at Plasmon wavelength was found to be linearly dependent on the concentration of GG-AuNPs, in accordance with the Beer-Lambert law (Figure s1(a)). Therefore, our results confirmed that the GG-AuNPs had excellent *in vitro* stability in simulated fluids at physiological pH, even under extreme dilutions [42].

Particles size analysis and Zeta potential measurement

Physicochemical properties, such as size, charge and morphology of gold Nanoparticles generated from GG, were determined by Uv-Visible spectroscopy, TEM, Dynamic Light Scattering (DLS) and zeta potential measurement. Uv-visible spectroscopy used to measure core size of gold Nanoparticles in solution and the surface plasmon resonance property of gold showed a peak within 500 nm to 600 nm. TEM was used to measure particle size of GG-AuNPs in dried state. DLS method was used to measure the hydrodynamic radius of GG-AuNPs in colloidal form as well as surface charge of GG-AuNPs. Our optimized GG-AuNPs preparation showed the λ_{max} at 555 nm. Based on Haiss equation particle size of gold Nanoparticles was measured [40].

The average particle size of 5-Fu@GG-AuNPs by DLS was found to be 588.1 nm as seen in Figure 3a. The increase in particle size is because of the coating of the particles by the water swellable guar gum. But Uv-visible spectra of GG-AuNPs showed an average particle size of 82 nm due do surface plasmon resonance of gold core Nanoparticles. Figure3b shows the zeta potential value of 5-Fu loaded polymer stabilized a gold nanoparticle which was found to be -3.18 (mV). TEM images show (Figure 3c) the external morphology of GG-AuNPs. The particles were found to be uniform in size and spherical in shape (black spots). The mean particle size of GG-AuNPs by TEM was found to be 12.78 ± 4.26 nm.

Loading efficiency and *in vitro* drug release kinetics

The site specific drug delivery to colon is important for the treatment of diseases associated with colon to reduce the dose and side effects of the administered drug. GG could potentially be used as a biodegradable material for the preparation of colon specific delivery systems of drugs that is not comfortable with stomach environments [24]. Intravenous administration of 5-Fu for colon cancer therapy could produce severe systemic side-effects due to its toxic effect on normal cells [32]. To avoid such problems, recently, GG tablet formulations were developed for site specific delivery of 5-Fu to the colon without the drug being released in the stomach or small intestine [25]. Compared to tablet formulation, Nanoparticles can enhance the efficiency of drug with minimum dose due to small size, higher permeation and muco-adhesiveness to target site [27]. The drug loading efficiency of GG-AuNPs was found to be 88.71 ± 1.2%.

In vitro release of 5-Fu-loaded AuNPs was performed under the pH 7.4. A controlled release profile was observed from GG-AuNPs (Figure 3d) GG used as carrier for 5-Fu@AuNPs. In the absence of enzyme system, the GG swells to form a viscous layer that slows down the seeping of the dissolution fluid into the core. The initial 6.56%

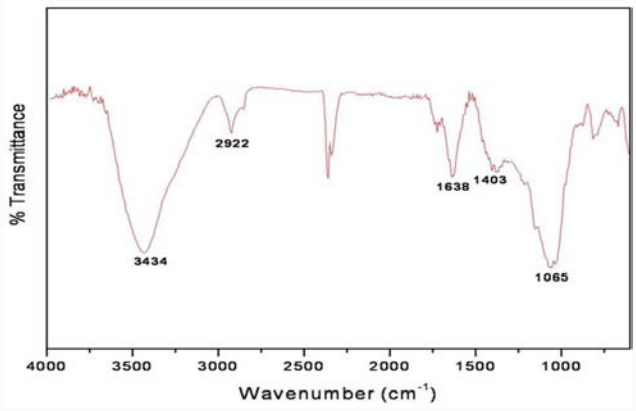

Figure S3: FTIR spectrum of 5-Fu.

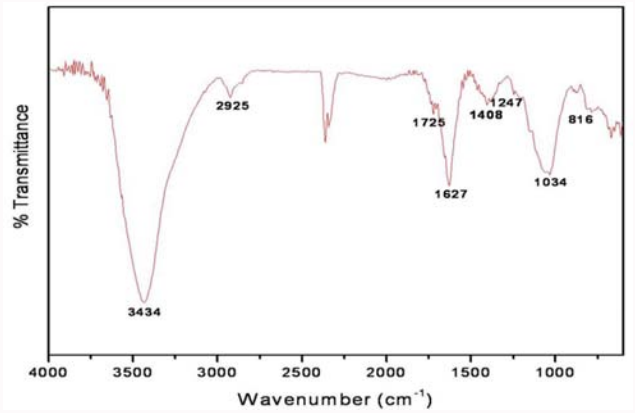

Figure S4: FTIR spectrum of 5-Fu@GG-AuNPs.

release can be attributed to the dissolution of drug present on the surface of GG-AuNPs.

From the release kinetics data of the slope and regression values, it is explained that the release of drug from GG-AuNPs follows the first order kinetics. The diffusion mechanism of drug release was further confirmed by the first order plots that showed fair linearity (R^2=0.9995), with a slope value of 0.1291, which was far less than 0.5, suggesting that the drug release mechanism was diffusion controlled.

FTIR analysis of nanoparticles

GG (Figure s2) exhibited characteristics bands at 3440 and 2928 cm^{-1} because of the O-H stretching vibrations of the polymer associated with C-H stretching vibrations. Additional characteristic absorption bands of GG appeared at 1437 and 1016 cm^{-1} because of C-H bending and O-H bending vibrations, respectively. As shown in Figure s3, the band at 3440 cm^{-1} shifted to 3434 cm^{-1} in the presence of gold, also the band was broader in GG compared to GG-AuNPs. These observations clearly indicated the interaction of gold Nanoparticles with the -OH group of GG. Similar results were reported earlier in the synthesis of silver Nanoparticles stabilized by Konjac Glucomannan, which is structurally similar to GG, by a photochemical reduction method [43].

Pure drug shows a band at 3300 cm^{-1} corresponding to the N-H stretching of secondary amine. Other absorption bands at 1700 and 1417 cm^{-1} are due to C=C and C–N stretching vibrations, respectively. The slight changes in the absorption frequencies observed in 5-Fu@ GG-AuNPs are because of the drug adsorbed on Nanoparticles (Figure 4).

Hemocompatibility of GG-AuNPs

In vitro studies on GG-AuNPs induced hemolysis can focus light on the behavior of the Nanoparticles under physiological conditions. Biocompatibility with blood cells is essential when Nanoparticles are used as carriers for drug delivery in *in-vivo* application. Figure 4a shows the hemolytic activities of GG-AuNPs dispersions with different concentrations. The results showed that % hemolytic activity of GG-AuNPs depended upon concentration. 0.85% hemolysis was observed when the concentration of GG-AuNPs was 0.018 mg/ml indicating that GG-AuNPs were suitable for *in vivo* application at a concentration 0.018 mg/ml.

Toxicity study of gold nanoparticles in zebrafish embryo model

Zebrafish embryos, possessing a high degree of homology to human genome, are a good choice for both *in vitro* and *in vivo* experiments for rapid high throughput and cost effective nanomaterials screening like dendrimers, silver and gold Nanoparticles [44]. So we have used this embryo model to screen the toxic effects of different concentrations of GG-AuNPs, 5-Fu@GG-AuNPs and 5-Fu. The toxicity of GG-AuNPs at different concentrations (0.003 mg, 0.006 mg, 0.009 mg, 0.012 mg, and 0.015 mg/ml) on zebrafish embryo was assessed by percentage survival rate (Figure 4a) and morphological analysis methods (Figure 4b). The GG-AuNPs was found to be less toxic up to a concentration of 0.003 mg/ml (83% of survival) which decreased to 18% at 0.015 mg/ml.

The LD_{50} value of this carrier was found to be 0.006 mg/ml (48%). The 5-Fu@GG-AuNPs with a concentration of 0.5 mg was found to be less toxic. This was confirmed by the percentage survival rate and morphological analysis methods. There are no morphological changes observed in the embryos in both GG-AuNPs and 5-Fu@GG-AuNPs. This was confirmed by the percentage survival rate (Figure 4c) and morphological analysis methods (Figure 4d).

Quantitative EAP Assay

Zebrafish is an excellent model for studying angiogenesis. It has a simple blood vessel system and can survive for several days without blood circulation. Angiogenic vessel growth can be monitored by Endogenous Alkaline Phosphatase (EAP) activity, which is present primarily in vessels during early development (before 72 hpf). The anti-angiogenic activity of 5-Fu@GG-AuNPs was compared with 5-Fu using zebrafish angiogenic assay. As shown in Figure 5a, 5-Fu and 5-Fu loaded GG-AuNPs showed anti-angiogenic activity in zebrafish model. Among them, 5-Fu loaded GG-AuNPs inhibited 35% of vessel formation at 0.5 mg and the inhibition reached 44% at 1.5 mg concentration. However, 5-Fu at 0.5 and 1.5 mg inhibited 22% and 25% of vessel formation respectively. This study indicated that the 5-Fu loaded GG-AuNPs has better anti-angiogenic activity.

In vitro cytotoxicity study

Using MTT assay, the cytotoxicity of free 5-Fu, 5-Fu@GG-AuNPs, against HT-29 cells was studied and shown in Figure 5b. The percentage of cell growth inhibition was measured by counting the cells after incubation for 24 hr. The 5-Fu concentration in all formulation was adjusted to be the same. The Ic_{50} values of 5-Fu, 5-Fu@GG-AuNPS, were 0.625 µg/ml (52%), 1.25 µg/ml (50.32 %), respectively. The amount of 5-Fu required to achieve 50% of growth of inhibition (Ic_{50}) for 5-Fu@GG-AuNPs was higher than 5-Fu due do slow release of 5-Fu from 5-Fu@GG-AuNPs. As the GG gum is

a colonic bacterial specific biopolymer, the polymer will degrade only in the presence of bacteria. In *in-vitro* condition, because of the absence of the bacterial enzymes, the polymer swells and becomes a viscous fluid due to its hydrophilic nature. Hence, the difference in the Ic_{50} may be due to the delayed drug release.

Conclusion

We developed a green chemistry microwave based method for synthesis of gold nanoparticles using a biopolymer, gaur gum for the first time. GG-AuNPs were physiologically stable and could carry 5-Fu to target colon cancer cell that over express galectine 1-s lectine receptor. The *in vitro* drug release and cytototoxicity efficacy results showed that 5-Fu@GG-AuNPs could be a promising alternative carrier for targeting colon cancer.

Acknowledgement

M. Ganeshkumar and T. Ponrasu would like to acknowledge the Council of Scientific and Industrial Research (CSIR), New Delhi, for granting Senior Research Fellowship and financial support. The authors thank Dr. M.D. Naresh (Biophysics Laboratory, CLRI) for the microscopic analyses. We acknowledge SAIF, IITM, Chennai for providing ICP-OES. The authors thank Central Instrumentation Lab, Tamilnadu Veterinary and Animal Science University for in the TEM analysis.

References

1. Ghazarian H, Idoni B, Oppenheimer SB. A glycobiology review: carbohydrates, lectins and implications in cancer therapeutics. Acta Histochem. 2011;113(3):236-47.
2. Dhas TS, Kumar VG, Karthick V, Govindaraju K, Narayana TS. Biosynthesis of gold nanoparticles using Sargassum swartzii and its cytotoxicity effect on HeLa cells. Spectrochim Acta A Mol Biomol Spectrosc. 2014;133:102-6.
3. Gerber A, Bundschuh M, Klingelhofer D, Groneberg DA. Gold nanoparticles: recent aspects for human toxicology. J Occup Med Toxicol. 2013;8(1):32.
4. Nghiem TH, La TH, Vu XH, Chu VH, Nguyen TH, Le QH, et al. Synthesis, capping and binding of colloidal gold nanoparticles to proteins. Adv Nat Sci Nanosci Nanotech.2010;1(2):025009.
5. Verma A, Stellacci F. Effect of surface properties on nanoparticle–cell interactions. Small. 2010;6(1):12-21.
6. Shemetov AA, Nabiev I, Sukhanova A. Molecular interaction of proteins and peptides with nanoparticles. ACS nano. 2012;6(6):4585-602.
7. Akhond M, Absalan G, Ershadifar H. Highly sensitive colorimetric determination of amoxicillin in pharmaceutical formulations based on induced aggregation of gold nanoparticles. Spectrochim Acta A Mol Biomol Spectrosc. 2015;143:223-9.
8. Sittiwong J, Unob F. Detection of urinary creatinine using gold nanoparticles after solid phase extraction. Spectrochim Acta A Mol Biomol Spectrosc. 2015;138 381-6.
9. Du J, Wang Y, Zhang W. Gold nanoparticles-based chemiluminescence resonance energy transfer for ultrasensitive detection of melamine. Spectrochim Acta A Mol Biomol Spectrosc. 2015;149:698-702.
10. Kim CJ, Lee DI, Kim C, Lee K, Lee CH, Ahn IS. Gold nanoparticles-based colorimetric assay for cathepsin B activity and the efficiency of its inhibitors. Anal Chem. 2014;86 (8):3825-33.
11. Dharmatti R, Phadke C, Mewada A, Thakur M, Pandey S, Sharon M. Biogenic gold nano-triangles: cargos for anticancer drug delivery. Mater Sci Eng C Mater Biol Appl. 2014;44:92-8.
12. Ganeshkumar M, Ponrasu T, Raja MD, Subamekala MK, Suguna L. Green synthesis of pullulan stabilized gold nanoparticles for cancer targeted drug delivery. Spectrochim Acta A Mol Biomol Spectrosc. 2014;130:64-71.
13. Ganeshkumar M, Sathishkumar M, Ponrasu T, Dinesh MG, Suguna L. Spontaneous ultra fast synthesis of gold nanoparticles using Punica granatum for cancer targeted drug delivery. Colloids Surf B Biointerfaces. 2013;106:208-16.
14. Khan MS, Vishakante GD, Siddaramaiah H. Gold nanoparticles: a paradigm shift in biomedical applications. Adv Colloid Interface Sci. 2013;199-200:44-58.
15. Murphy CJ, Jana NR. Controlling the Aspect Ratio of Inorganic Nanorods and Nanowires. Adv Mater. 2002;14:80-2.
16. Daniel MC, Astruc D. Gold Nanoparticles: assembly, supramolecular chemistry, quantum-size related properties, and applications towards biology, catalysis and nanotechnology. Chem Soc Rev. 2004;104(1):293-346.
17. Brown KR, Walter DG, Natan MJ. Seeding of Colloidal Au Nanoparticle Solutions. 2. Improved Control of Particle Size and Shape. Chem Mater. 2000;12:306-13.
18. Han MY, Quek CH. Photochemical Synthesis in Formamide and Room-Temperature Coulomb Staircase Behavior of Size-Controlled Gold Nanoparticles. Langmuir. 2000;16:362-7.
19. Chen H, Zou H, Paholak HJ, Ito M, Qian W, Che Y, et al. Thiol-reactive amphiphilic block copolymer for coating gold nanoparticles with neutral and functionable surfaces. Polym Chem. 2014;5(8):2768-73.
20. Rastogi L, Kora AJ, J A. Highly stable, protein capped gold nanoparticles as effective drug delivery vehicles for amino-glycosidic antibiotics. Mater Sci Eng C Mater Biol Appl 2012;32(6):1571-7.
21. Jia L, Guo L, Zhu J, Ma Y. Stability and cytocompatibility of silk fibroin-capped gold nanoparticles. Mater Sci Eng C Mater Biol Appl. 2014;43:231-6.
22. Manju V, Dhandapani P, Gurusamy Neelavannan M, Maruthamuthu S, Berchmans S, et al. Tunable release of clavam from clavam stabilized gold nanoparticles--design, characterization and antimicrobial study. Mater Sci Eng C Mater Biol Appl. 2015;49:500-8.
23. Goldstein AM, Alter EN, Seaman JK. Guar gum. In: Whistler RL, Editor. Industrial gums, polysaccharides their derivatives. New York: Academic Press. 1973;303-21.
24. Baweja JM, Misra AN. Modified guar gum as a tablet disintegrant. Pharmazie. 1997;52:856-9.
25. Bayliss CE, Houston AP. Characterization of plant polysaccharide- and mucin-fermenting anaerobic bacteria from human feces. Appl Environ Microbiol. 1984;48:626-32.
26. Tomolin J, Taylor JS, Read NW. The effects of mixed bacteria on a selection of viscous polysaccharides in vitro. Nutr Rep Int. 1989;39:121-35.
27. Krishnaiah YS, Satyanarayana S, Rama Prasad YV, Narasimha Rao S. Gamma scintigraphic studies on guar gum matrix tablets for colonic drug delivery in healthy human volunteers. J Control Release. 1998;55(2-3):245-52.
28. Dodi G, Pala A, Barbu E, Peptanariu D Hritcu D, Popa MI, et al. Carboxymethyl guar gum nanoparticles for drug delivery applications: Preparation and preliminary *in-vitro* investigations. Mater Sci Eng C Mater Biol Appl. 2016:63:628-36.
29. Choi IS, Oh DY, Kim BS, Lee KW, Kim JH, Lee JS. Oxaliplatin, 5-FU, folinic acid as first-line palliative chemotherapy in elderly patients with metastatic or recurrent gastric cancer. Cancer Res Treat. 2007;39:99-103.
30. Kim JS, Kim JS, Cho MJ, Yoon WH, Song KS. Comparison of the efficacy of oral capecitabine versus bolus 5-FU in preoperative radiotherapy of locally advanced rectal cancer. J Korean Med Sci. 2006;21:52-7.

31. Wang JM, Xiao BL, Zheng JW, Chen HB, Zou SQ. Effect of targeted magnetic nanoparticles containing 5-FU on expression of bcl-2, bax and caspase 3 in nude mice with transplanted human liver cancer. World J Gastroenterol. 2007;13(23):3171-5.

32. Diasio RB, Harris BE. Clinical pharmacology of 5-fluorouracil. Clin Pharmacokinet. 1989;16:215-37.

33. Wei H, Qing D, De-Ying C, Bai X, Li-Fang F. *In-vitro* and *in-vivo* studies of pectin/ethylcellulosefilm-coated pellets of 5-fluorouracil for colonic targeting. J Pharm Pharmacol. 2008;60(1)35-44.

34. Rahman Z, Kohli K, Khar RK, Ali M, Charoo NA, Shamsher AA. Characterization of 5-fluorouracil microspheres for colonic delivery. AAPS Pharm Sci Tech. 2006;7(2):E47-E53.

35. Raj Kumar S, Akanksha T. Carbohydrate polymers; Applications and recent advances in delivering drugs to the colon. Carbohydr Polym. 2012;88:399-16.

36. Laroui H, Dalmasso G, Nguyen HT, Yan Y, Sitaraman SV. Drug-loaded nanoparticles targeted to the colon with polysaccharide hydrogel reduce colitis in a mouse model. Gastroenterol. 2010;138(3):843-53.

37. Gajalakshmi B, Induja S, Sivakumar N, Raghavan P. Guar Gum Stabilized Copper Oxide Nanoparticles with Enhanced Thermal and Antimicrobial Properties. Asian J Chem. 2018;30(5): 1099-101.

38. Balachandramohan J, Anandan S, Sivasankar T. A simple approach for the sonochemical synthesis of Fe3O4-guargum nanocomposite and its catalytic reduction of p-nitroaniline. Ultrason Sonochem. 2018;40(Pt A):1-10.

39. Liu X, Jin Q, Ji Y, Ji J. Minimizing nonspecific phagocytic uptake of biocompatible gold nanoparticles with mixed charged zwitterionic surface modification. J Mater Chem. 2012;22:1916-27.

40. Parng C, Seng WL, Semino C, McGrath P. Zebrafish: a preclinical model for drug screening. Assay Drug Dev Technol. 2002;1:41-8.

41. Nune SK, Chanda N, Shukla R, Katti K, Kulkarni RR, Thilakavathi S, et al. Green Nanotechnology from Tea: Phytochemicals in Tea as Building Blocks for Production of Biocompatible Gold Nanoparticles. J Mater Chem. 2009;19:2912-20.

42. Haiss W, Thanh NT, Aveyard J, Fernig DG. Determination of size and concentration of gold nanoparticles from UV-vis spectra. Anal Chem. 2007;79(11):4215-21.

43. Dating T, Weibing H, Zhen Z, Hangbao L, Hong-Quan X. Study on in situ synthesis of konjac glucomannan/silver nanocomposites via photochemical reduction. J Appl Polym Sci. 2006;100(2):1323-7.

44. Heiden TC, Dengler E, Kao WJ, Heideman W, Peterson RE. Developmental toxicity of low generation PAMAM dendrimers in zebrafish. Toxicol Appl Pharmacol. 2007;225(1):70-9.

45. Bar-Ilan O, Albrecht RM, Fako VE, Furgeson DY. Toxicity assessments of multisized gold and silver nanoparticles in zebrafish embryos. Small. 2009;5(16):1897-910.